Mid-infrared semiconductor laser based trace gas sensor technologies: recent advances and applications

RICE

F.K.Tittel, W. Ren, W. Jiang, Y. Cao and D. Jiang
Department of Electrical and Computer Engineering,
Rice University, Houston, TX 77005, USA

http://www.ece.rice.edu/~lasersci/

OUTLINE

CUHK, 20th Anniversary

Hong Kong, China

August 29, 2014

- New Laser Based Trace Gas Sensor Technology
  - Novel Multipass Gas Absorption Cells & Electronics
  - Quartz Enhanced Photoacoustic Spectroscopy
- Examples of nine mid-infrared Trace Gas Species
  - C_2H_6, NH_3, NO, CO, SO_2, CH_4, N_2O, H_2O_2 & C_3H_6O
- Future Directions of Laser Based Gas Sensor Technology and Conclusions

Research support by NSF ERC MIRTHE, NSF-ANR NexCILAS, the Robert Welch Foundation, and Sentinel Photonics Inc. via an EPA Phase 1 SBIR sub-award is acknowledged

Wide Range of Trace Gas Sensing Applications

- **Urban and Industrial Emission Measurements**
  - Industrial Plants
  - Combustion Sources and Processes (e.g. fire detection)
  - Automobile, Truck, Aircraft and Marine Emissions
- **Rural Emission Measurements**
  - Agriculture & Forestry, Livestock
- **Environmental Monitoring**
  - Atmospheric Chemistry (e.g isotopologues, climate modeling,…)
  - Volcanic Emissions
- **Chemical Analysis and Industrial Process Control**
  - Petrochemical, Semiconductor, Pharmaceutical, Metals Processing, Food & Beverage Industries, Nuclear Technology & Safeguards
- **Spacecraft and Planetary Surface Monitoring**
  - Crew Health Maintenance & Life Support
- **Applications in Medical Diagnostics and the Life Sciences**
- **Technologies for Law Enforcement, Defense and Security**
- **Fundamental Science and Photochemistry**

RICE

"Curiosity" Landed on Mars on August 6, 2012

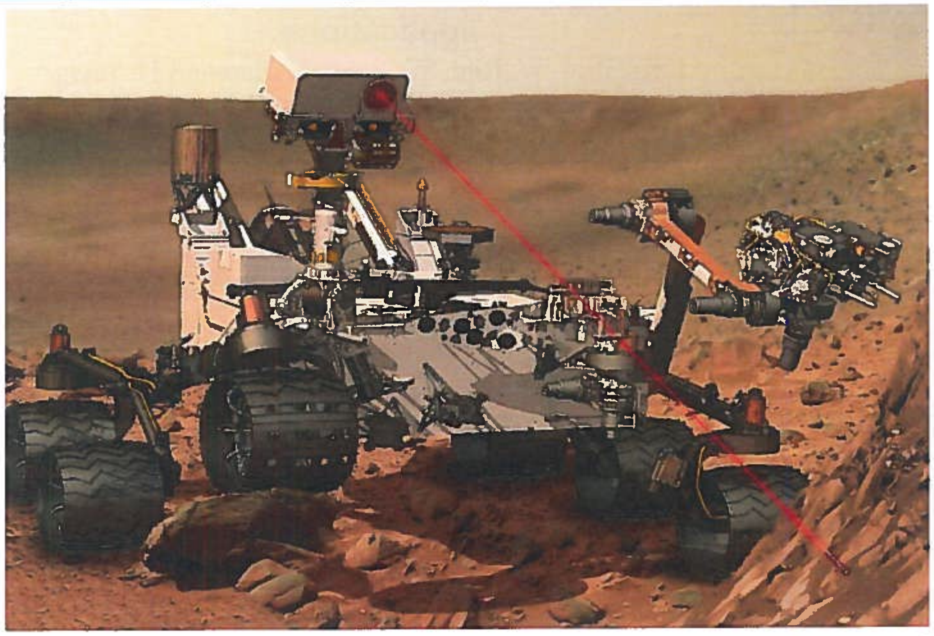

Laser based Trace Gas Sensing Techniques

- **Optimum Molecular Absorbing Transition**
  - Overtone or Combination Bands (NIR)
  - Fundamental Absorption Bands (Mid-IR)
- **Long Optical Pathlength**
  - Multipass Absorption Cell (White, Herriot, Chernin, Sentinel Photonics)
  - Cavity Enhanced and Cavity Ringdown Spectroscopy
  - Open Path Monitoring (with retro-reflector): Standoff and Remote Detection
  - Fiberoptic Evanescent Wave Spectroscopy
- **Spectroscopic Detection Schemes**
  - Frequency or Wavelength Modulation
  - Balanced Detection
  - Zero-air Subtraction
  - Photoacoustic & Quartz Enhanced Photoacoustic Spectroscopy (QEPAS)

RICE

Other Spectroscopic Methods

- Faraday Rotation Spectroscopy (limited to paramagnetic chemical species)
- Differential Optical Dispersion Spectroscopy (DODiS)
- Noise Immune Cavity Enhanced-Optical Heterodyne Molecular Spectroscopy (NICE-OHMS)
- Frequency Comb Spectroscopy
- Laser Induced Breakdown Spectroscopy (LIBS)

RICE

HITRAN Simulated Mid-Infrared Molecular Absorption Spectra

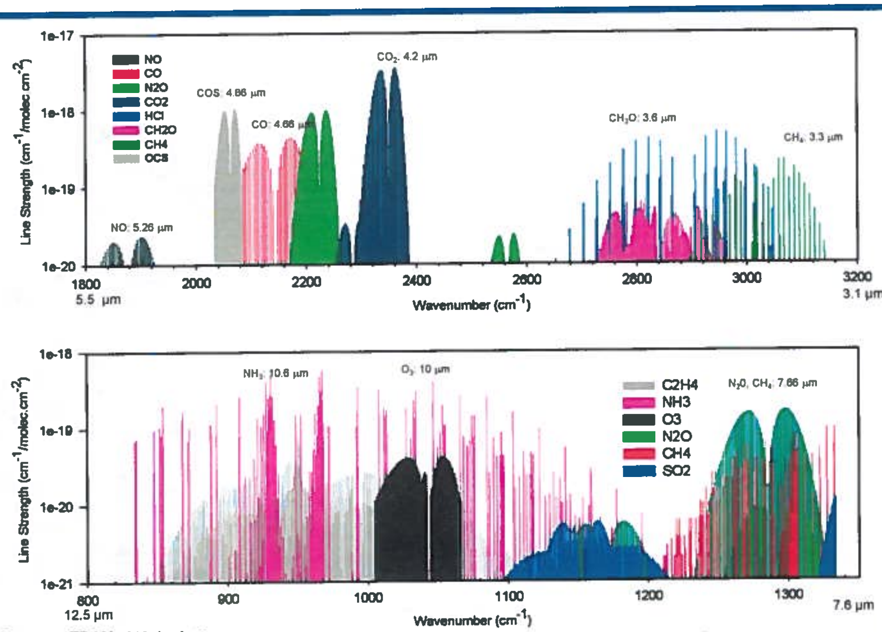

Source: HITRAN 2012 database

RICE

Mid-IR Source Requirements for Laser Spectroscopy

REQUIREMENTS	IR LASER SOURCE
Sensitivity (% to pptv)	Optimum Wavelength, Power
Selectivity (Spectral Resolution)	Stable Single Mode Operation and Narrow Linewidth
Multi-gas Components, Multiple Absorption Lines and Broadband Absorbers	Mode Hop-free Wavelength Tunability
Directionality or Cavity Mode Matching	Beam Quality
Rapid Data Acquisition	Fast Time Response
Room Temperature Operation	High wall plug efficiency, no cryogenics or cooling water
Field deployable in harsh environments	Compact & Robust

Key Characteristics of Mid-IR QCL & ICL Sources – Aug 2014

- **Band – structure engineered devices**
  Emission wavelength is determined by layer thickness – MBE or MOCVD; Type I QCLs operate in the 3 to 24 µm spectral region; Type II and GaSb based ICLs can cover the 3 to 6 µm spectral range.
  - Compact, reliable, stable, long lifetime, and commercial availability
  - Fabry-Perot (FP), single mode (DFB) and multi-wavelength devices

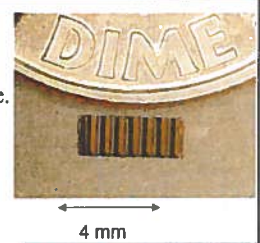

- **Wide spectral tuning ranges in the mid-IR**
  - 1.5 cm^{-1} using injection current control for DFB devices
  - 10-20 cm^{-1} using temperature control for DFB devices
  - ~100 cm-1 using current and temperature control for QCL DFB Array
  - ~ 525 cm^{-1} (22% of c.w.) using an external grating element and FP chips with heterogeneous cascade active region design; also QCL DFB Array

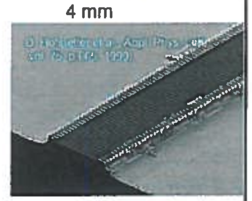

- **Narrow spectral linewidths**
  - CW: 0.1 - 3 MHz & <10kHz with frequency stabilization (0.0004 cm^{-1})
  - Pulsed: ~ 300 MHz
- **High pulsed and CW powers of QCLs at TEC/RT temperatures**
  - Room temperature pulsed power of > 30 W with 44% wall plug efficiency and CW powers of ~ 5 W with 23% wall plug efficiency at 293 °K
  - > 1W, TEC CW DFB @ 4.6 µm ~~EC-QCLs & ICLs~~
  - > 600 mW (CW [illegible] @ RT; wall plug efficiency of ~[illegible]% at 4.6 µm;

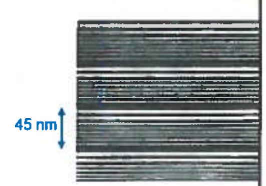

~ DFB @ 285K   23%

Motivation for Mid-infrared C_2H_6 Detection

- **Application in medical breath analysis**
  - Asthma
  - Schizophrenia
  - Lung cancer
  - Vitamin E deficiency
- **Atmospheric chemistry and climate**
  - Fossil fuel and biofuel consumption
  - Biomass burning
  - Vegetation/soil
  - Natural gas loss

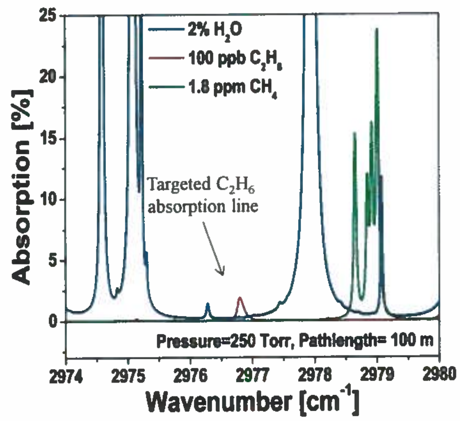

HITRAN absorption spectra of C_2H_6, CH_4, and H_2O

RICE

C_2H_6 Detection with a 3.36 μm CW DFB LD using a Novel Compact Multipass Absorption Cell and Control Electronics

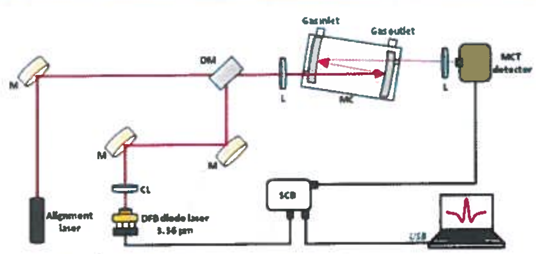

Schematic of a C_2H_6 gas sensor using a Nanoplus 3.36 μm DFB laser diode. M – mirror, CL – collimating lens, DM – dichroic mirror, MC – multipass cell, L – lens, SCB – sensor control board.

Innovative long path, small volume multipass gas cell: **57.6 m with 459 passes**

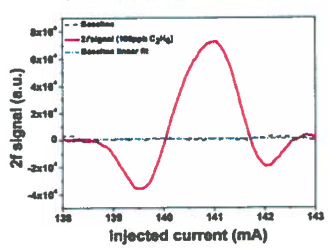

2f WMS signal for a C_2H_6 line at 2976.8 cm^{-1} at 200 Torr

Minimum detectable C_2H_6 concentration:
~ 740 pptv (1σ; 1 s time resolution)

MGC dimensions: **17 x 6.5 x 5.5 (cm)**
Distance between the MGC mirrors: 12.5 cm

10

Motivation for NH_3 Detection

- **Medical diagnostics**
  - Kidney disease
  - Liver failure and Cirrhosis
  - Brain Cells dysfunction
  - Drowsiness and Coma
- **Atmospheric chemistry**
- **Pollutant gases monitoring**
- **Monitoring NH_3 concentrations in the exhaust stream of NO_x removal systems based on selective catalytic reduction (SCR) techniques associated with electric power plants**
- **Spacecraft related trace gas monitoring**

RICE

Conventional Photoacoustic Spectroscopy (PAS)

Cell is OPTIONAL!

***V*-effective volume**

Laser beam, power *P*

Modulated (P or λ) at f or $f/2$

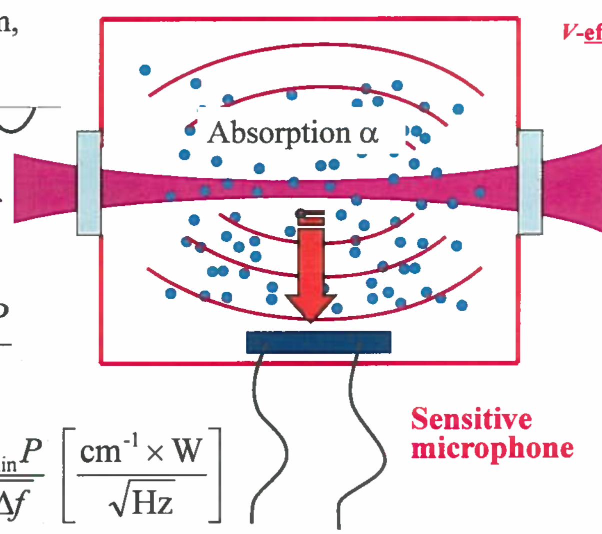

$$S \sim \frac{Q \alpha P}{f V}$$

$$NNEA = \frac{\alpha_{min} P}{\sqrt{\Delta f}} \left[\frac{cm^{-1} \times W}{\sqrt{Hz}} \right]$$

RICE

Unexpected Remote detection of

Atmospheric NH_3 Measurements using an EC-QCL PAS Sensor

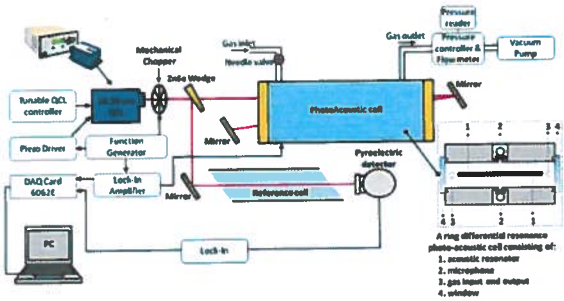

Schematic of a Daylight Solutions 10.36 µm CW TEC EC-QCL based PAS NH_3 Sensor.

NH_3 sensor deployed at the UH Moody Tower rooftop monitoring site.

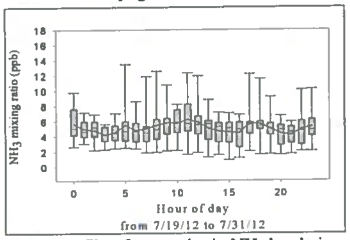

Diurnal profile of atmospheric NH_3 levels in Houston, TX.

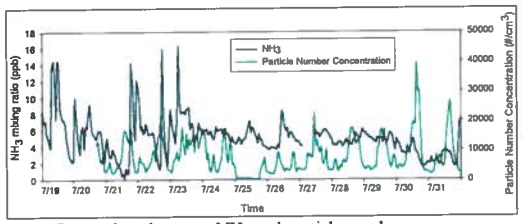

Comparison between NH_3 and particle number concentration time series from July 19 to July 31 2012.

NH_3 Detection due to a Fire resulting from a Truck Collision

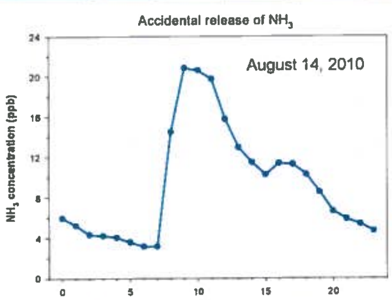

A chemical incident occurred at ~ 6 a.m. after two trucks collided on I-59. Both trucks caught fire. [www.chron.com]

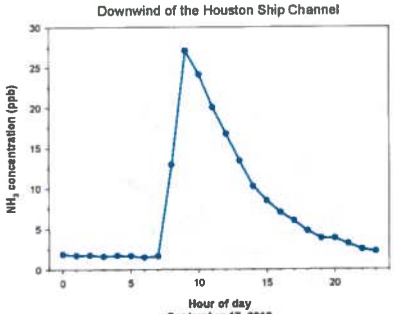

Estimated hourly NH_3 emission from the Houston Ship Channel area is about 0.25 ton. Mellqvist et al., (2007) Final Report, HARC Project H-53.

RICE

14

Sporadic increase in NH_3 concentration levels related to emissions by the Parish Electric Power Plant, TX

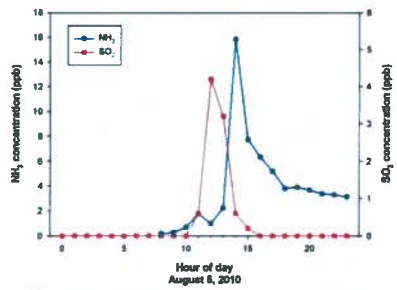

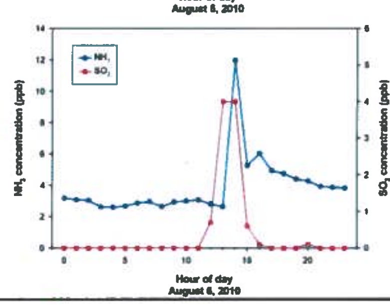

The Parish electric power plant is located near the Brazos River in Fort Bend County, Texas (~27 miles SW from downtown Houston)

RICE

Fort-Worth, Dallas(TX) CAMS 75 & TCEQ monitoring site

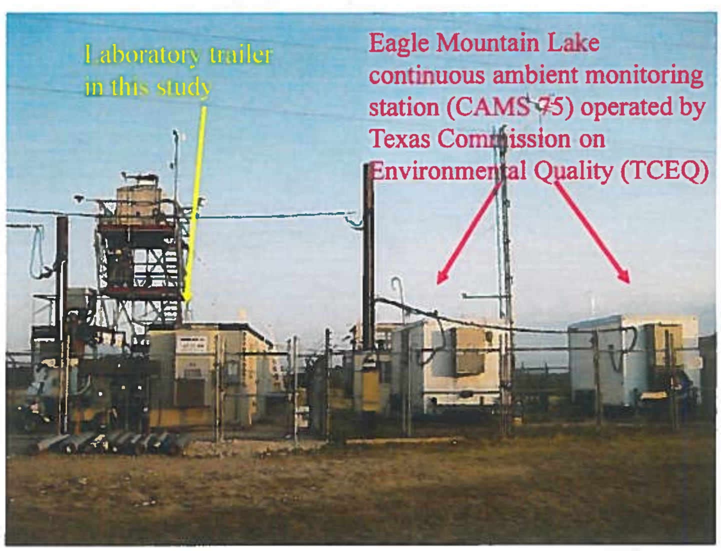

RICE

16

Instrumentation available at CAMS 75 & TCEQ monitoring site

Species/parameter	Measurement technique
NH_3	Daylight Solutions External Cavity Quantum Cascade Laser (Photo-acoustic Spectroscopy)
CO	Thermo Electron Corp. 48C Trace Level CO Analyzer (Gas Filter Correlation)
SO_2	Thermo Electron Corp. 43C Trace Level SO_2 Analyzer (Pulsed Fluorescence)
NO_x	Thermo Electron Corp. 42C Trace Level NO-NO_2-NO_X Analyzer (Chemiluminescence)
NO_y	Thermo Electron Corp. 42C-Y NO_Y Analyzer (Molybdenum Converter)
HNO_3	Mist Chamber coupled to Ion Chromatography (Dionex, Model CD20-1)
HCl	Mist Chamber coupled to Ion Chromatography (Dionex, Model CD20-1)
VOC_s	IONICON Analytik Proton Transfer Reaction Mass Spectrometer and TCEQ Automated Gas Chromatograph
PBL height	Vaisala Ceilometer CL31 with updated firmware to work with Vaisala Boundary Layer View software
Temperature	Campbell Scientific HMP45C Platinum Resistance Thermometer
Wind speed	Campbell Scientific 05103 R. M. Young Wind Monitor
Wind direction	Campbell Scientific 05103 R. M. Young Wind Monitor

RICE

NH_3 Source Attribution & Temperature Variations

- Emission events from specified point sources (i.e., industrial facilities)
- Estimated NH_3 emissions from cows (1.3 tons/day)
- Estimated NH_3 emissions from soil and vegetation (0.15 tons/day)
- EPA PMF (biogenic:74.1%; light duty vehicles:12.1%; natural gas/industry: 9.4%; heavy duty vehicles:4.4%)
- Livestock might account for approximately 66.4% of total NH_3 emissions
- Increased contribution from industry (→18.9%)

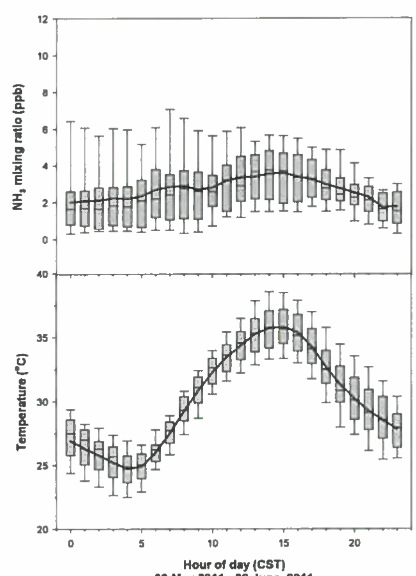

18

From Conventional **PAS** to Quartz Enhanced PAS **(QEPAS)**

Laser beam, power *P*

Modulated (P or λ) at f or $f/2$

$$S \sim \frac{Q \alpha P}{f V}$$

$$NNEA = \frac{\alpha_{min} P}{\sqrt{\Delta f}} \left[\frac{cm^{-1} \times W}{\sqrt{Hz}} \right]$$

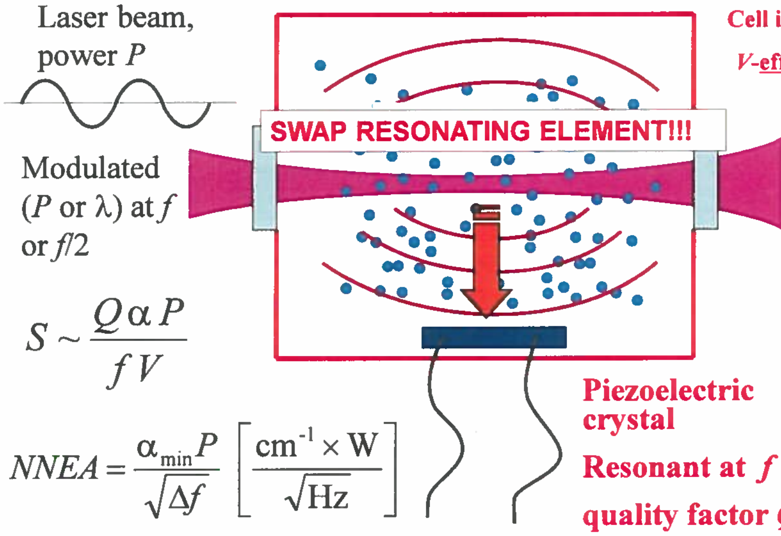

Q>>1000

Cell is OPTIONAL!

V-effective volume

Piezoelectric crystal

Resonant at f

quality factor Q

RICE

Quartz Tuning Fork as a Resonant Microphone for QEPAS

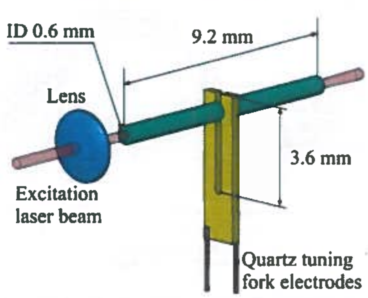

Unique Properties

- Extremely low internal losses:
  - Q~10 000 at 1 atm
  - Q~100 000 in vacuum
- Acoustic quadrupole geometry
  - Low sensitivity to external sound
- Large dynamic range (~10^6) – linear from thermal noise to breakdown deformation
  - 300K noise: $x \sim 10^{-11}$ cm
  - Breakdown: $x \sim 10^{-2}$ cm
- Wide temperature range: from 1.6K to ~700K

Acoustic Micro-resonator (μR) Tubes

- Optimum inner diameter: 0.6 mm; μR-QTF gap is 25-50 μm
- Optimum mR tubes must be ~ 4.4 mm long (~$\lambda/4 < l < \lambda/2$ for sound at 32.8 kHz)
- SNR of QTF with μR tubes: ×30 (depending on gas composition and pressure)

20

Optimum NH_3 Line Selection for a 10.34 μm CW TEC DFB QCL

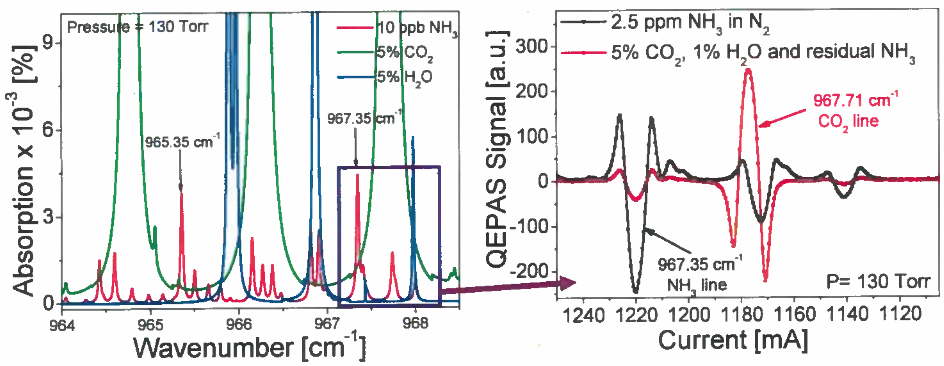

Simulated HITRAN high resolution spectra @ 130 Torr indicating two NH_3 absorption lines of interest

No overlap between NH_3 and CO_2 absorption lines was observed for the selected **967.35 cm⁻¹** NH_3 absorption line in the ν_2 R-band.

RICE

QEPAS based NH_3 Gas Sensor Architecture

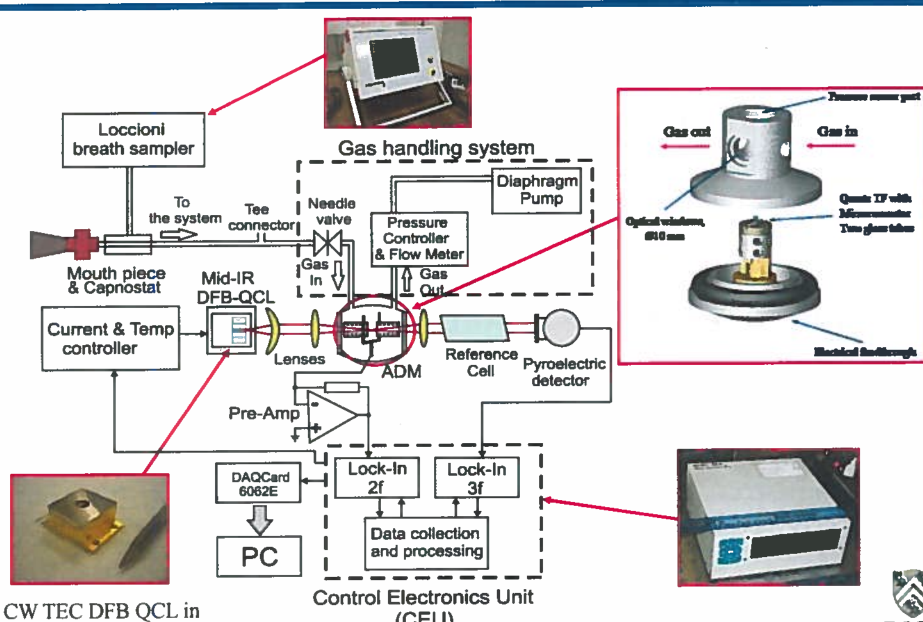

CW TEC DFB QCL in HHL package (Hamamatsu)

RICE

22

Real-time exhaled human NH_3 Breath Measurements

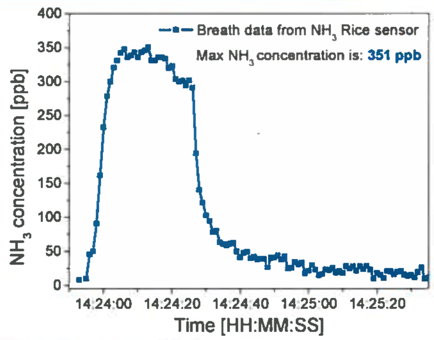

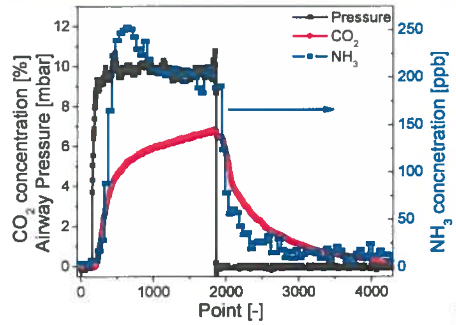

Airway pressure (black), CO_2 (red), and NH_3 (blue) profiles of a single breath exhalation lasting 40sec.

Successful testing of a 2nd generation breath ammonia monitor installed in a clinical environment.(Johns Hopkins, Baltimore, MD and St. Luke's Hospital, Bethlehem, PA)

Minimum detectable concentration of NH_3 is:
~ 6 ppbv at 967.35 cm^{-1} (1σ; 1 s time resolution)

Motivation for Nitric Oxide Detection

- **NO in medicine and biology**
  - Important signaling molecule in physiological processes in humans and mammals (1998 Nobel Prize in Physiology/Medicine)
  - Treatment of asthma, chronic obstructive pulmonary disease (COPD) & lung rejection
- **Environmental pollutant gas monitoring**
  - Ozone depletion
  - Precursor of smog and acid rain
  - NO_X monitoring from automobile exhaust and power plant emissions
- **Atmospheric Chemistry**

RICE

24

Molecular Absorption Spectra within two Mid-IR Atmospheric Windows and NO absorption @ 5.26µm

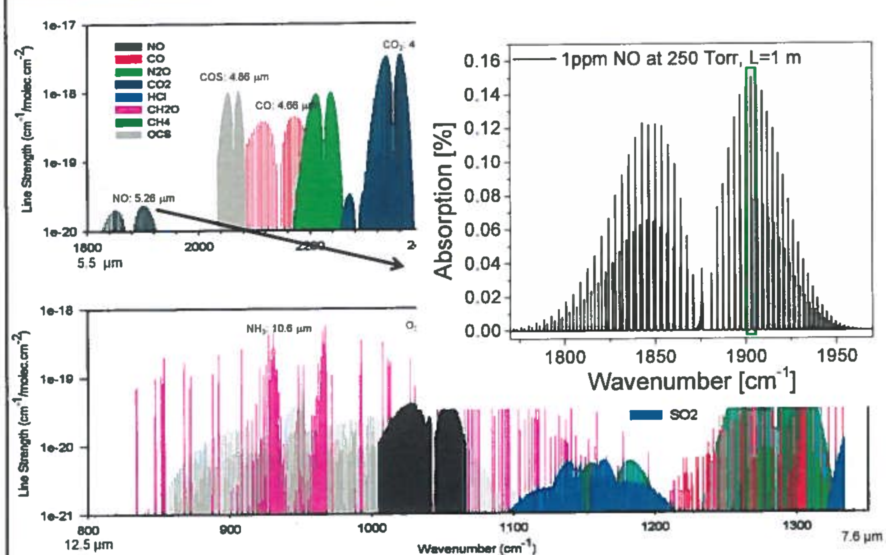

Source: HITRAN 2012 database

RICE

Emission spectra of a 1900cm^{-1} TEC DFB QCL and HITRAN simulated spectra of NO, H_2O & CO_2

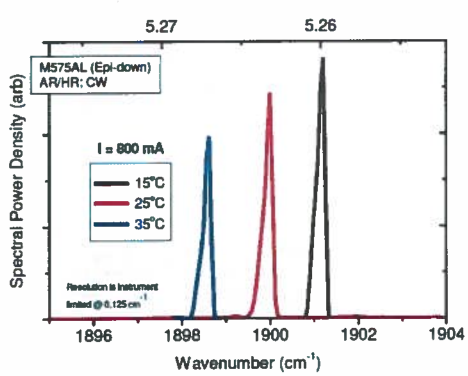

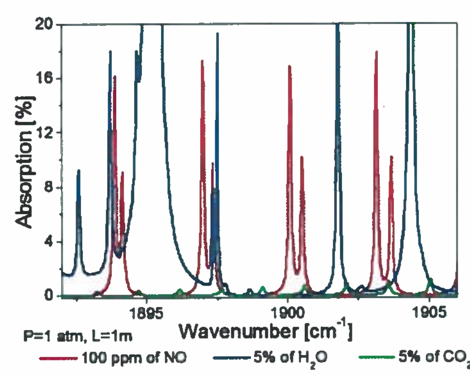

Output power: 117 mW @ 25 C
Thorlabs/Maxion

RICE

26

Performance of a 5.26 μm CW HHL TEC DFB-QCL

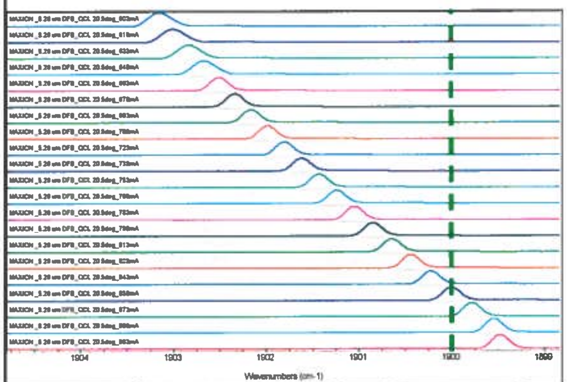

Single frequency QCL radiation recorded with FTIR for different laser current values at a QCL temperature of 20.5°C.

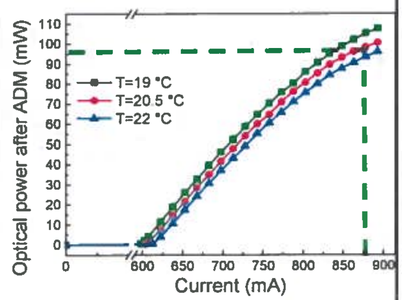

CW DFB-QCL optical power and current tuning at three different temperatures.

RICE

CW TEC DFB QCL based QEPAS NO Gas Sensor

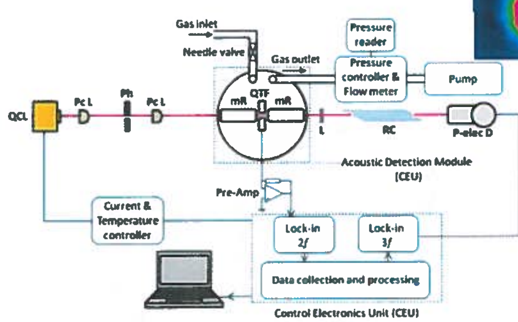

Schematic of a DFB-QCL based Gas Sensor.
PcL – plano-convex lens, Ph – pinhole,
QTF – quartz tuning fork, mR – microresonator,
RC- reference cell, P-elec D – pyro electric detector

CW HHL TEC DFB-QCL package and IR camera image of the laser beam at 630 mA and 20.5 deg C through tubes after ADM

Compact Prototype NO Sensor (September 2012)

RICE

Performance of CW DFB-QCL based WMS QEPAS NO Sensor Platform

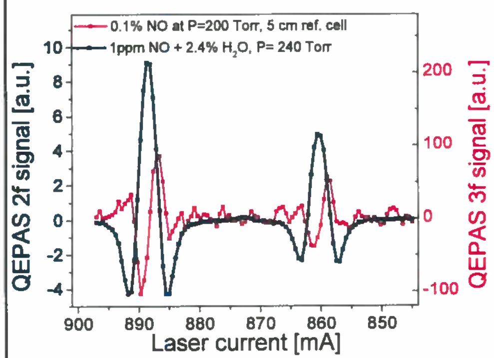

2f QEPAS signal (navy) and reference 3f signal (red) when DFB-QCL was tuned across **1900.08 cm⁻¹** NO line.

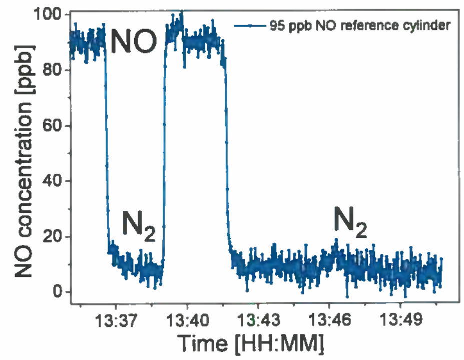

2f QEPAS signal amplitude for 95 ppb NO when DFB-QCL was locked to the **1900.08 cm⁻¹** line.

Minimum detectable NO concentration is:

~ 3 ppbv (1σ; 1 s time resolution)

RICE

QCL based TDLAS Sensor for Detection of NO Emission from Cancer Cells

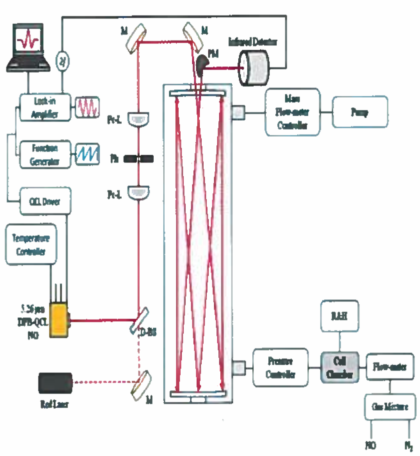

Schematic drawing of the sensor setup

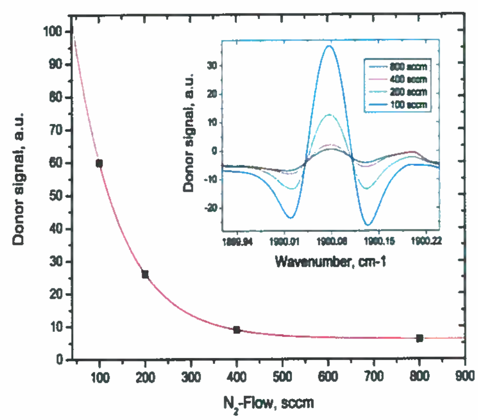

Dependence of the sensor signal from biological samples on the overall gas flow of the sensor system (black squares). The inset shows spectra corresponding to the data points.

30

Motivation for Carbon Monoxide Detection

- **CO in Medicine and Biology**
  - Hypertension and abnormality in heme metabolism
- **Public Health**
  - Extremely dangerous to human life even at a low concentrations. Therefore CO must be carefully monitored at low concentration levels (<35 ppm).
- **Atmospheric Chemistry**
  - Incomplete combustion of natural gas, fossil fuel and other carbon containing fuels.
  - Impact on atmospheric chemistry through its reaction with hydroxyl (OH) for troposphere ozone formation and changing the level of greenhouse gases (e.g. CH_4).

RICE

Performance of a 4.61µm high power CW TEC DFB QCL

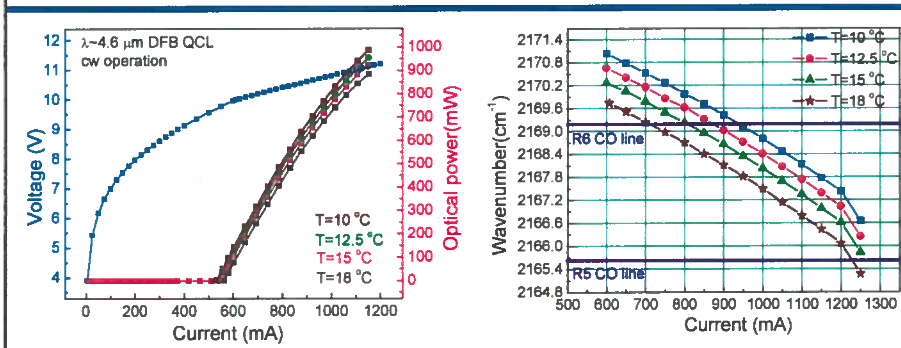

CW DFB-QCL optical power and current tuning at a four different QCL temperatures.

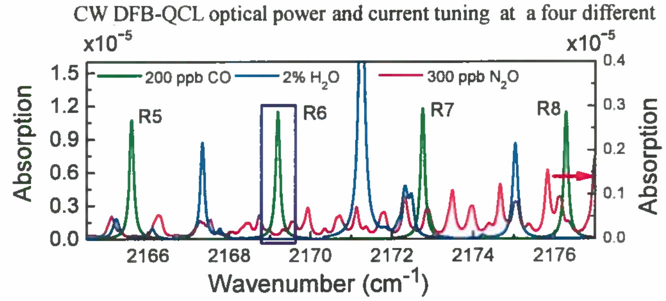

Estimated max wall-plug efficiency (WPE) is ~ 7% at 1.25A QCL drive-current.

RICE

32

CW DFB-QCL based CO QEPAS Sensor Results

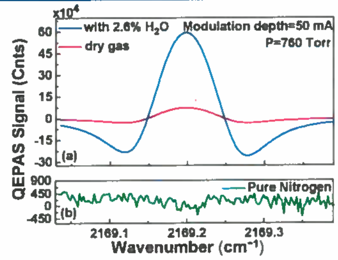

2f QEPAS signal for dry (red) and moisturized (blue) 5 ppm CO:N_2 mixture near **2169.2 cm^{-1}**.

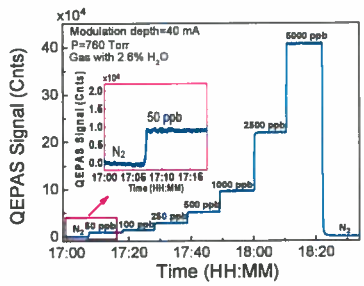

Dilution of a 5 ppm CO reference gas mixture when the CW DFB-QCL is locked to the **2169.2 cm^{-1}** R6 CO line.

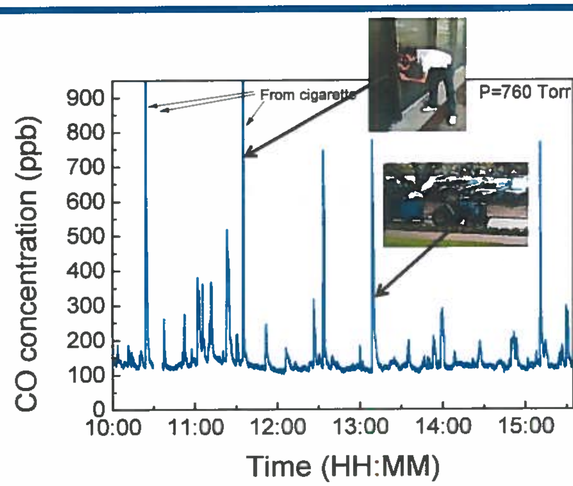

Atmospheric CO concentration levels on Rice University campus, Houston, TX

Minimum detectable CO concentration is:

~ 2 ppbv (1σ; 1 s time resolution)

RICE

CW DFB-QCL based SO_2 QEPAS Results

Motivation for Sulfur Dioxide Detection

- SO_2 exposure affects lungs and causes breathing difficulties, bronchitis, cardiovascular disease
- Currently, reported annual average atmospheric SO_2 concentrations range from ~ 1 - 6 ppb
- Prominent air pollutant
- Emitted from coal fired power plants (~73%) and other industrial facilities (~20%)
- In the atmosphere SO_2 converts to sulfuric acid ➔ primary contributors to acid rain
- SO_2 reacts to form sulfate aerosols
- Primary SO_2 exposure for 1 hour is 75 ppb

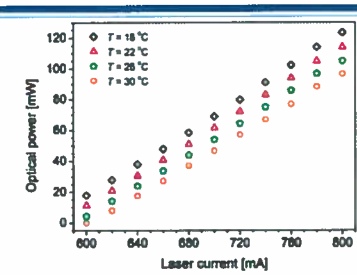

7.24 µm CW DFB-QCL optical power and current tuning at three different operating temperatures.

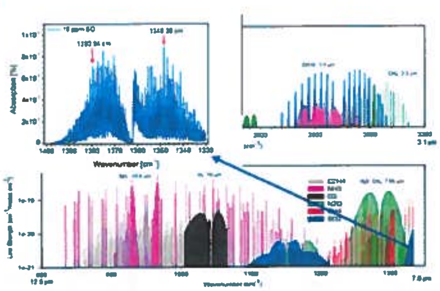

Molecular Absorption Spectra within two Mid-IR Atmospheric Windows

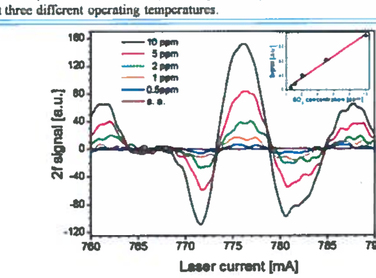

2f WMS QEPAS signals for different SO_2 concentrations when laser was tuned across **1380.9 cm^{-1}** line.

Minimum detectable SO_2 concentration is:

~ 100 ppbv (1σ; 1 s time resolution)

34

QEPAS based CH_4 and N_2O Gas Sensor

Motivation for CH_4 and N_2O Detection

- Medical Diagnostics
  - Nausea, blurred vision, vomiting
- Prominent greenhouse gases
- Sources: wetlands, leakage from natural gas systems, fossil fuel production and agriculture

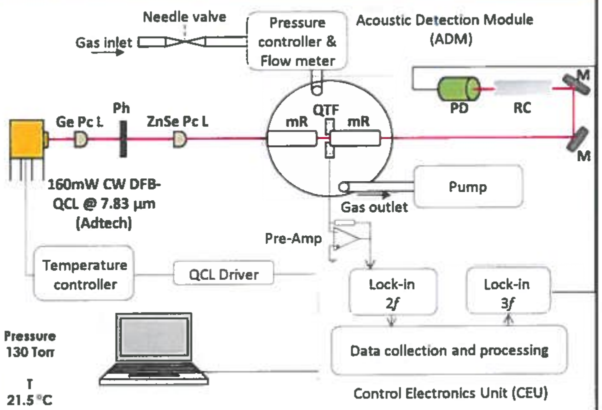

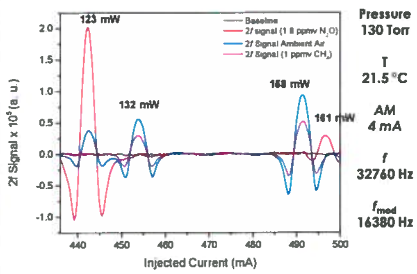

The Analyst Aug. 2013

Detection Limit (1σ) with a **1-sec** averaging time
Methane (CH_4) (1275.04 cm^{-1}) **13 ppbv**
Nitrous Oxide (N_2O) (1275.5 cm^{-1}) **6 ppbv**

Deduced N_2O concentration in the ambient laboratory air: **331 ppbv**

RICE

CH_4 Measurements performed with a DFB-QCL based QEPAS Sensor installed in Aerodyne Mobile Laboratory (Sept 7, 2013)

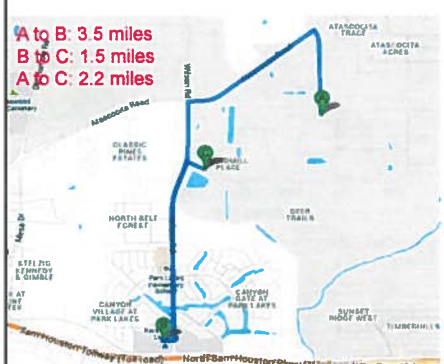

Atascocita Landfill, Humble, TX 77396
CH4 Perimeter Measurements

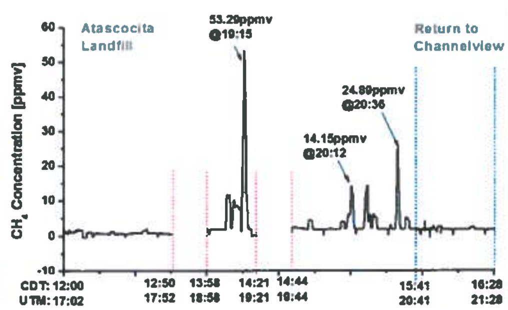

A: 29.9599° North, 95.2334° West
B: 29.9364° North, 95.2508° West
C: 29.9547° North, 95.2462° West (Landfill)

Jahjah et. al., Opt. Let., 39, 957-960, 2014

36

QCL based QEPAS Sensor for Hydrogen Peroxide (H_2O_2)

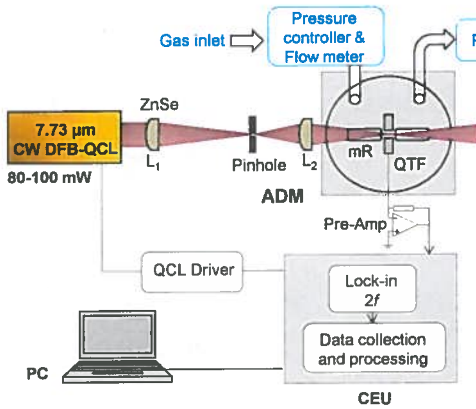

Schematic of QCL based QEPAS sensor: ADM – acoustic detection module; CEU – control electronics unit; PC – personal computer.

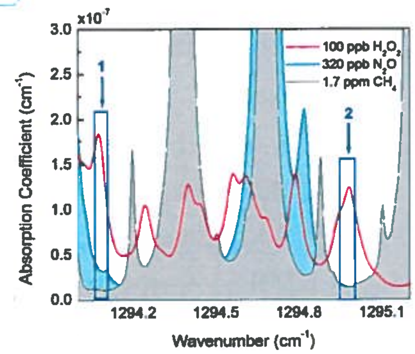

Simulated spectra (HITRAN) of H_2O_2 at 296 K and 130 Torr, along with atmospheric interfering molecules of CH_4 and N_2O; two target wavelengths at 1294.1 and 1294.9 cm^{-1} are shown.

RICE

H_2O_2 Exposure limit is set at 1 ppmv by OSHA

38

QEPAS Performance for Trace Gas Species (August 2014)

	Molecule (Host)	Frequency, cm^{-1}	Pressure, Torr	NNEA, $cm^{-1}W/Hz^{½}$	Power, mW	NEC (τ=1s), ppmv
VIS	O_3 (air)	35087.70	700	3.0×10^{-8}	0.8	1.27
VIS	O_2 (N_2)	13099.30	158	4.74×10^{-7}	1228	13
NIR	C_2H_2 (N_2)*	6523.88	720	4.1×10^{-9}	57	0.03
NIR	NH_3 (N_2)*	6528.76	575	3.1×10^{-9}	60	0.06
NIR	C_2H_4 (N_2)*	6177.07	715	5.4×10^{-9}	15	1.7
NIR	CH_4 (N_2+1.2% H_2O)*	6057.09	760	3.7×10^{-9}	16	0.24
NIR	N_2H_4	6470.00	700	4.1×10^{-8}	16	1
NIR	H_2S (N_2)*	6357.63	780	5.6×10^{-9}	45	5
NIR	HCl (N_2 dry)	5739.26	760	5.2×10^{-8}	15	0.7
NIR	CO_2 (N_2+1.5% H2O) *	4991.26	50	1.4×10^{-8}	4.4	18
Mid-IR	CH_2O (N_2:75% RH)*	2804.90	75	8.7×10^{-9}	7.2	0.12
Mid-IR	CO (N_2 +2.2% H_2O)	2176.28	100	1.4×10^{-7}	71	0.002
Mid-IR	CO (propylene)	2196.66	50	7.4×10^{-8}	6.5	0.14
Mid-IR	N_2O (air+5%SF_6)	2195.63	50	1.5×10^{-8}	19	0.007
Mid-IR	C_2H_5OH (N_2)**	1934.2	770	2.2×10^{-7}	10	90
Mid-IR	NO (N_2+H_2O)	1900.07	250	7.5×10^{-9}	100	0.003
Mid-IR	C_2HF_5 (N_2)***	1208.62	770	7.8×10^{-9}	6.6	0.009
Mid-IR	NH_3 (N_2)*	1046.39	110	1.6×10^{-8}	20	0.006
Mid-IR	SF_6	948.62	75	2.7×10^{-10}	18	5×10^{-5} (50 ppt)

* - Improved microresonator
** - Improved microresonator and double optical pass through ADM
*** - With amplitude modulation and metal microresonator

NNEA – normalized noise equivalent absorption coefficient.
NEC – noise equivalent concentration for available laser power and τ=1s time constant, 18 dB/oct filter slope

For comparison: conventional PAS 2.2×10^{-9} $cm^{-1}W/\sqrt{Hz}$ for NH_3

Future Directions and Outlook

- New target analytes: formaldehyde (CH_2O), ethylene (C_2H_4), ozone (O_3), nitrate (NO_3),
- Ultra-compact, low cost, robust sensors (e.g. C_2H_6, NO, CO…) CH_4
- QCL based ultra-portable atmospheric carbon isotope monitor for $^{12}CH_4$ & $^{13}CH_4$
- Monitoring of broadband absorbers: acetone (C_3H_6O)-, ~ MDL:1.5 ppm with a 7mW ICL & AM, or 20ppb with a 100mW QCL @ 8.23µm; benzene (C_6H_6)…
- Optical power build-up cavity designs (I-QEPAS)
- THz QEPAS based sensors
- Development of trace gas sensor networks

RICE

40

Why is THz important for gas sensing ?

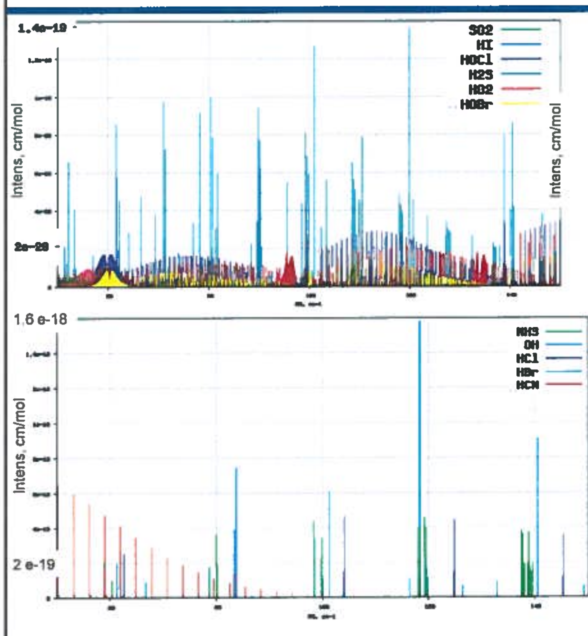

Several gas species such as HF, OH, HCN, HCL, HBr, NH_3, H_2O_2, H_2S, H_2O, explosive (vapor phase) show strong absorption bands in the THz spectral region

Mainly rotational levels are involved in THz absorption processes and rotational-translational (R-T) relaxation rates are up to ***three order of magnitude faster*** with respect to vibrational-translational (V-T) relaxation rates.

Source: HITRAN 2000 database

Why is THz important for gas sensing ?

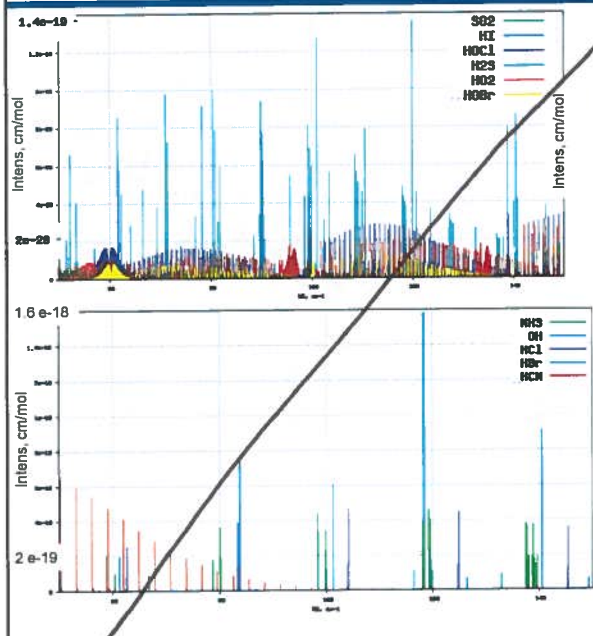

Source: HITRAN 2000 database

Several gas species such as HF, OH, HCN, HCL, HBr, NH_3, H_2O_2, H_2S, H_2O, explosive (vapor phase) show strong absorption bands in the THz spectral region

Mainly rotational levels are involved in THz absorption processes and rotational-translational (R-T) relaxation rates are up to ***three order of magnitude faster*** with respect to vibrational-translational (V-T) relaxation rates.

Why QEPAS sensors have not been developed in the THz range to-date?

Standard QTFs and are characterized by a very small sensitive volume (~0.3×0.3×3 mm³)

In QEPAS experiments, it is critical to avoid laser illumination of the QTF, since the radiation blocked by the QTF prongs results in an undesirable non-zero background which is associated with a shifting fringe- like interference pattern.

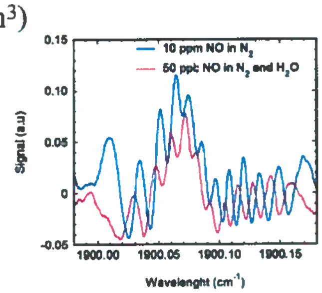

The narrow space (300 µm) between the QTF prongs is comparable with the wavelength of THz sources, which has so far represented the main limitation preventing the use of QEPAS system in THz range.

Hence, larger sized QTFs are required for operating in the THz regime.

42

Custom QTFs can be scaled in dimension with respect to a standard 32.76 KHz QTF (7 and 3 times larger) for THz trace gas sensing

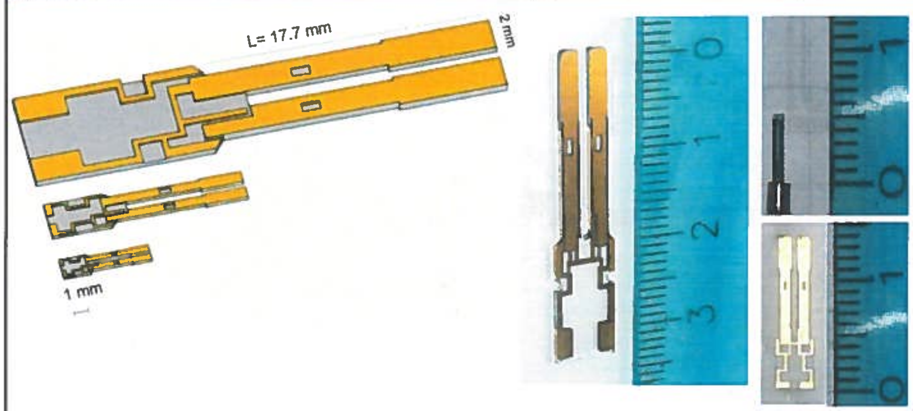

- Standard photolithographic techniques can be used to etch custom QTFs, starting from a z-cut quartz wafer.
- Chromium/gold contacts can be deposited on both sides of a QTF.

RICE

THz QEPAS based Sensor for Methanol (CH_3OH) Detection

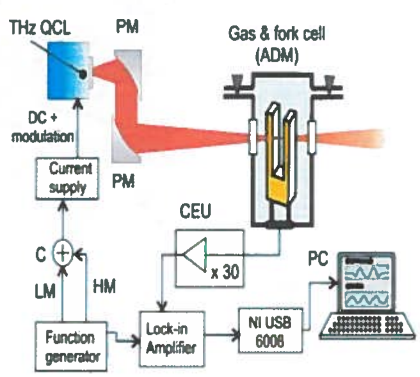

Schematic of THz QCL-based QEPAS sensor. PM – paraboloidal mirror; C – power combiner; LM, HM – low-frequency modulation (triangular ramp), high-frequency modulation; CEU – control electronics unit; PC – personal computer.

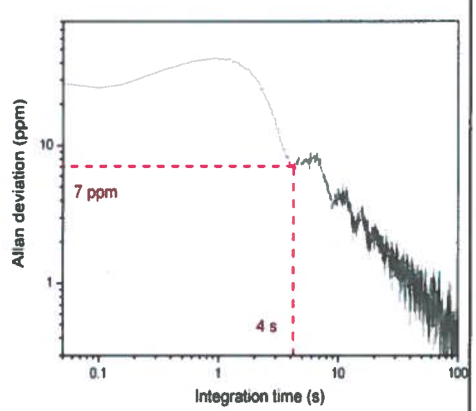

Allan deviation in ppm of the QEPAS signal as a function of the integration time. The initial growth from 0.1 to 1s reflects delays due to the signal sampling time (200 ms).

Spangolo et. al. Appl. Phys. Lett. **103**, 021105 (2013)

RICE

44

Performance of mid-infrared gas sensing techniques

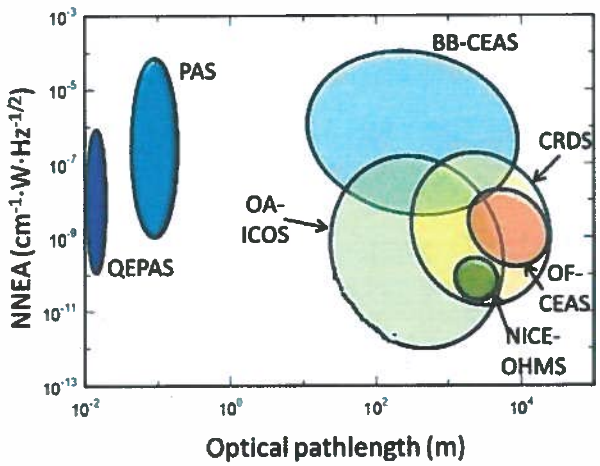

NNEA for categories of gas detection techniques as a function of optical path-length. Key: BB- CEAS— broadband cavity-enhanced spectroscopy, CRDS—cavity ring-down spectroscopy, OA-ICOS—off- axis integrated cavity output spectroscopy, OF-CEAS—optical feedback cavity-enhanced absorption spectroscopy, NICE-OHMS—noise-immune cavity-enhanced optical heterodyne spectroscopy, PAS photoacoustic spectroscopy, QEPAS—Quartz-enhanced photoacoustic spectroscopy.

P. Patimisco, G. Scamarcio, F.K. Tittel & V. Spagnolo, "Quartz-enhanced photoacoustic spectroscopy: a review", Sensors, 14, 6165-6206, (2014)

Proposed Intracavity-QEPAS (I-QEPAS) Sensor System

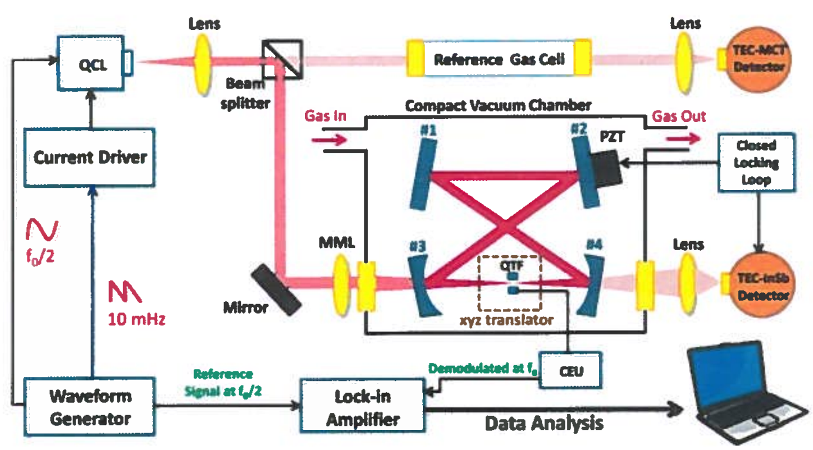

Optical power build up cavity can provide:

- RT CW DFB QCL, λ=4.33 microns
- Low noise current driver → narrow QC laser linewidth ~1 MHz
- Bow-tie cavity →4 high reflectivity mirrors, R=99.9%
- Electronic Control Loop + PZT motor lock to cavity resonant frequecny to QCL frequency

P. Patimisco, G. Scamarcio, F.K. Tittel & V. Spagnolo, "Quartz-enhanced photoacoustic spectroscopy: a review", Sensors, 14, 6165-6206 (2014)

46

Optical Properties of I-QEPAS Bow-Tie Cavity

Cavity response:

- Voltage ramp + **modulation dither** applied to QCL
- under vacuum
- locking loop ON

$f_0/2$ + 10 mHz

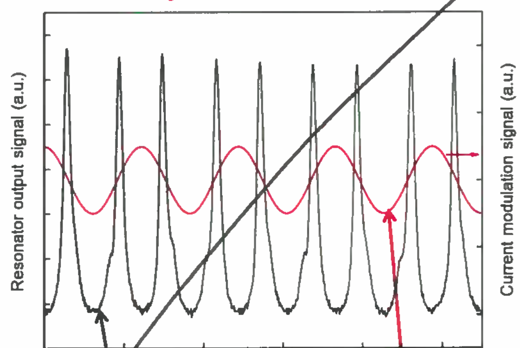

Cavity response

Sinusoidal dither at $f_0/2$ = 16 kHz

- The close-locked loop acts on the PZT tuning the cavity length
- It was not fast enough to follow the fast dither at $f_0/2$ = 16 kHz
- It maintains the optical cavity resonant with the laser frequency at the center of the fast dither

Mechanical chopper at f_0

Optical Properties of I-QEPAS Bow-Tie Cavity (cont.)

Cavity response:

- Voltage ramp + **modulation dither** applied to QCL
- under vacuum
- locking loop ON

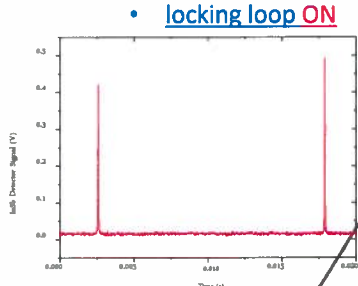

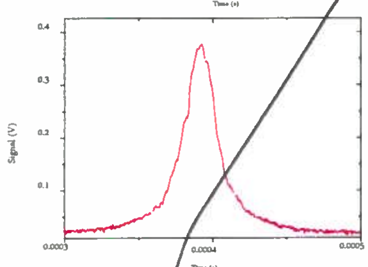

Cavity length L = 174mm

FSR = c/L = 1.725 GHz

Δν(FWHM)= 1.15 MHz

F = FSR/ Δν = 1505

G = F/π= 480

Mode matching 50%

Intracavity optical power enhancement factor = 240

Comparison of I-QEPAS with Other Trace Gas Sensing Techniques

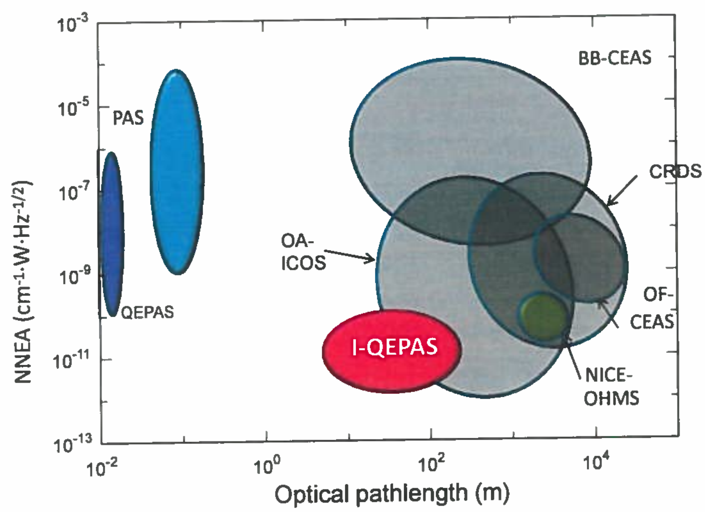

P. Patimisco, G. Scamarcio, F.K. Tittel & V. Spagnolo, "Quartz-enhanced photoacoustic spectroscopy: a review", Sensors, 14, 6165-6206 (2014)

Potential Integration of a CW DFB- QCL and QEPAS Absorption Detection Module

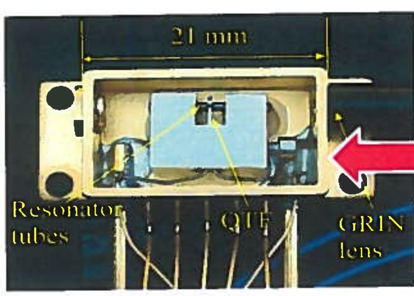

2012 QEPAS ADM

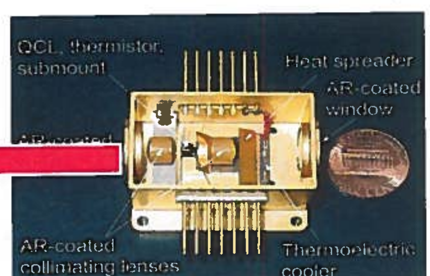

HHL package fiber coupled DFB-QCL

A. Lyakh, et al "1.6 W high wall plug efficiency, continuous-wave room temperature quantum cascade laser emitting at 4.6 μm", Appl. Phys. Lett. 92, 111110 (2008)

48

Summary and Conclusions

- Development of robust, compact, sensitive, selective mid-infrared trace gas sensor technology based on room temperature, continuous wave DFB laser diodes and high performance QCLs for medical diagnostics and environmental monitoring.
- Interband cascade and quantum cascade lasers were used in TDLAS, PAS and QEPAS based sensor platforms
- Six target trace gas species were detected with a 1 sec sampling time:
  - C_2H_6: ~3.36 µm, detection sensitivity of 740 pptv using TDLAS
  - NH_3: ~10.4 µm, detection sensitivity of ~1 ppbv (200 sec averaging time)
  - NO: ~5.26 µm, detection limit of 3 ppbv
  - CO: ~4.61 µm, minimum detection limit of 2 ppbv
  - SO_2: ~7.24 µm, detection limit of 100 ppbv
  - CH_4 and N_2O: ~7.28 µm, detection limits of 13 and 6 ppbv, respectively
  - H_2O_2: ~7.73 µm, detection limit of 75 ppb
  - C_2H_6O:
- New target analytes: CH_2O, C_6H_6, and C_3H_8

RICE

Merits of QEPAS based Trace Gas Detection

- Very small sensing module and sample volume (a few mm^3 to ~2cm^2)
- Extremely low dissipative losses
- Optical detector is not required
- Wide dynamic range
- Frequency and spatial selectivity of acoustic signals
- Rugged transducer – quartz monocrystal; can operate in a wide range of pressures and temperatures
- Immune to environmental acoustic noise, sensitivity is limited by the fundamental thermal TF noise: k_BT energy in the TF symmetric mode
- Absence of low-frequency noise: SNR scales as $\sqrt{t}$, up to t=3 hours as experimentally verified

QEPAS: some challenges

- Cost of Spectrophone assembly
- Sensitivity scales with laser power
- Effect of H_2O
- Responsivity depends on the speed of sound and molecular energy transfer processes
- Cross sensitivity issues

RICE